



The photophysics of a Rhodamine head labeled phospholipid in the identification and characterization of membrane lipid phases

Bruno M. Castro^{a,*}, Rodrigo F.M. de Almeida^{b,1}, Aleksander Fedorov^a, Manuel Prieto^a

^a Centro de Química Física-Molecular and Institute of Nanoscience and Nanotechnology, Instituto Superior Técnico, Universidade Técnica de Lisboa, Av. Rovisco Pais, 1049-001 Lisboa, Portugal

^b Centro de Química e Bioquímica, Faculdade de Ciências da Universidade de Lisboa, Campo Grande, 1749-016 Lisboa, Portugal

ARTICLE INFO

Article history:

Received 28 January 2012

Received in revised form 21 February 2012

Accepted 22 February 2012

Available online 3 March 2012

Keywords:

Membrane domains

Cholesterol

Liquid-disordered phase

Liquid-ordered phase

Gel phase

Fluorescence

ABSTRACT

The organization of lipids and proteins into domains in cell membranes is currently an established subject within biomembrane research. Fluorescent probes have been used to detect and characterize these membrane lateral heterogeneities. However, a comprehensive understanding of the link between the probes' fluorescence features and membrane lateral organization can only be achieved if their photo-physical properties are thoroughly defined. In this work, a systematic characterization of *N*-(lyssamine Rhodamine B sulfonyl)-1,2-dioleoyl-*sn*-3-phosphatidylethanolamine (Rhod-DOPE) absorption and fluorescence behavior in gel, liquid-ordered (l_o) and liquid-disordered (l_d) model membranes was performed. In agreement with a previous study, it was found that Rhod-DOPE fluorescence lifetimes present a strong sensitivity to lipid phases, becoming significantly shorter in l_o membranes as the probe membrane concentration increases. The sensitivity of Rhod-DOPE absorption and fluorescence properties to the membrane phase was further explored. In particular, the fluorescence lifetime sensitivity was shown to be a consequence of the enhanced Rhod-DOPE fluorescence dynamic self-quenching, due to the formation of probe-rich membrane domains in these condensed phases that cannot be considered as typical probe aggregates, as excitonic interaction is not observed. The highly efficient dynamic self-quenching was shown to be specific to l_o phases, pointing to an important effect of membrane dipole potential in this process. Altogether, this work establishes how to use Rhod-DOPE fluorescence properties in the study of membrane lipid lateral heterogeneities, in particular cholesterol-enriched lipid rafts.

© 2012 Elsevier Ireland Ltd. All rights reserved.

1. Introduction

Lipid lateral organization into different types of domains and the role that these domains have in several cellular processes is one of the most important topics in current lipid research (Bagatolli et al., 2010; Simons and Gerl, 2010). However, this subject has been difficult to tackle. It is necessary to apply careful, systematic and highly controlled approaches that go through the comparison of cell studies with membrane model systems experiments (Bastos et al., 2012; Stockl et al., 2008). Advances in this subject are intimately

related with the development of tools to probe lipid membrane organization and dynamics.

Due to their unique self-quenching properties, Rhodamine (Rhod)-based probes have been used in fusion assays (e.g. (Aroeti and Henis, 1987; Hoekstra and Klappe, 1986; Stegmann et al., 1986)). In addition, since it was found that the enhanced self-quenching displayed by these molecules in lipid membranes extracted from Sendai virus (Aroeti and Henis, 1987) was due to the presence of cholesterol (Chol) (MacDonald, 1990), Rhod-labeled lipids have been extensively used in the study of membrane lateral organization (de Almeida et al., 2007, 2005; Juhasz et al., 2010, 2011; Loura et al., 1996, 2001). This type of probes has been useful to address the properties of membranes displaying fluid/gel coexistence (Juhasz et al., 2011), and also in Förster resonance energy transfer (FRET) studies (usually as acceptors to NBD-labeled donor lipids) regarding the size of liquid-ordered cholesterol-enriched domains in binary phosphatidylcholine (PC)/Chol mixtures (Loura et al., 2001) and in the raft system PC/sphingomyelin/Chol in the absence and presence of the raft-marker ganglioside G_{M1} (de Almeida et al., 2005). Furthermore, these probes were valuable in the study of ceramide interactions with lipid rafts (Silva

Abbreviations: Chol, cholesterol; DOPC, 1,2-dioleoyl-*sn*-glycero-3-phosphocholine; DPPC, 1,2-dipalmitoyl-*sn*-glycero-3-phosphocholine; l_d , liquid-disordered; LUV, large unilamellar vesicles; l_o , liquid-ordered; MLV, multilamellar vesicles; PC, phosphatidylcholine; POPC, 1-palmitoyl-2-oleoyl-*sn*-glycero-3-phosphocholine; Rhod-DOPE, *N*-(lyssamine Rhodamine B sulfonyl)-1,2-dioleoyl-*sn*-3-phosphatidylethanolamine; FRET, Förster resonance energy transfer.

* Corresponding author. Tel.: +351 218419248; fax: +351 218464455/57.

E-mail address: bruno.castro@ist.utl.pt (B.M. Castro).

¹ Equally contributing authors.

et al., 2007) and their effects on Fas transmembrane domain membrane organization (Castro et al., 2011). Due to their small Stoke's shift, Rhod-probes have a high critical radius for homo-FRET (energy migration), which combined with its high anisotropy allows addressing membrane structure properties without the need for another probe (de Almeida et al., 2007). Rhodamine-lipids, owing to their high photostability and emission in visible wavelengths, have also been used in microscopy experiments, namely in two-photon microscopy (Bagatolli and Gratton, 2000), as well as in fluorescence lifetime imaging microscopy (de Almeida et al., 2007). Because these probes have been widely used in different types of photophysical experiments, being able to detect and characterize different types of lipid domains/phases, they have a great potential in the era of lipidomics (van Meer, 2005). In this context, the photophysical properties of well-characterized fluorescent probes can be used to laterally solve the lipid domains in membranes of cells (not only plasma membrane but also organelle membranes), and also to infer about the lipid composition of those domains, or at the least about the composition alterations undergone in response to the eliciting of different cellular processes.

However, in order to achieve the ultimate goal mentioned above, it is necessary that the approach be systematic to allow a correct interpretation of the experimental data. In the present work we characterize the absorption, steady-state and time-resolved fluorescence intensity and steady-state fluorescence anisotropy of *N*-(1-lyssamine Rhodamine B sulfonyl)-1,2-dioleoyl-*sn*-3-phosphatidylethanolamine (Rhod-DOPE) at room temperature in both aqueous solution and lipid membranes in the following phases: (i) a 1,2-dipalmitoyl-*sn*-glycero-3-phosphocholine (DPPC) gel; (ii) a typical DPPC/Chol liquid-ordered (l_o) phase (Davis et al., 2009; Vist and Davis, 1990); (iii) a "weak interaction 1-palmitoyl-2-oleoyl-*sn*-glycero-3-phosphocholine (POPC)/Chol l_o phase" (de Almeida et al., 2003); and (iv) liquid-disordered (l_d) phases composed of either 1,2-dioleoyl-*sn*-glycero-3-phosphocholine (DOPC), DOPC/Chol or POPC (Davis et al., 2009; de Almeida et al., 2007, 2003). We discuss the differences in the photophysical behavior of Rhod-DOPE in each system, highlighting its useful properties for the study of membrane lipid lateral assemblies. Moreover, the l_o/l_d partition coefficient for the POPC/Chol system was determined. From the collected data, it is concluded that the increased self-quenching of Rhodamine-labeled phospholipid requires not only the presence of cholesterol, but in fact the formation of a condensed l_o phase.

2. Materials and methods

2.1. Chemicals

DOPC, DPPC, POPC and Rhod-DOPE were purchased from Avanti Polar Lipids (Birmingham, AL). Cholesterol was purchased from Sigma (St. Louis, MO). All other reagents were of the highest purity available.

2.2. Liposome preparation

Multilamellar vesicles (MLV) containing the appropriate lipids and Rhod-PE were prepared by standard procedures (e.g. Reyes Mateo et al., 1993). Briefly, adequate volumes of lipids and probe stock solutions were added to a glass tube in order to have the desired lipid mole fractions and lipid/probe ratio. The solvent was slowly vaporized by a mild flow of nitrogen, forming a thin layer of lipid in the bottom of the tube that was left under high vacuum overnight to ensure the complete removal of the organic solvents. The lipid was hydrated with HEPES buffer 10 mM pH 7.4 200 mM NaCl previously heated above T_m of DPPC. The samples were then progressively vortex-stirred and submitted to freeze/thaw cycles

(liquid nitrogen/water bath at 60 °C). Afterwards, they were slowly cooled and kept overnight in the dark at 4 °C. Before measurements, they were slowly brought to room temperature. The probe/lipid ratio was varied from 1/2000 to 1/25 and the total lipid concentration was 0.5 mM. In this way, the results are shown as a function of total probe concentration (in μM), but this is easily converted to mole fraction in the membrane (this was in general varied from 0.05 mol% up to 4 mol%). As a consequence of the preparation procedure, the probe is evenly distributed between the two bilayer leaflets. Large unilamellar vesicles (LUV) were obtained by the extrusion method (de Almeida et al., 2005). Briefly, the MLV suspension obtained as described above was forced through a pair of polycarbonate filters with pore diameter of 0.1 μm 21 times, in an Avanti Mini-Extruder (Avanti Polar Lipids). DPPC, DOPC and POPC concentration in stock solutions and in liposome suspensions were determined using inorganic phosphate colorimetric quantification (McClare, 1971). Cholesterol concentration in stock solutions was determined by gravimetry (Mettler Toledo UMT2).

2.3. Absorption spectroscopy

Absorption spectroscopy data were obtained with a Shimadzu UV-3101PC spectrophotometer. Measurements were performed in 1 cm quartz absorption cells. Probe concentration in stock solution was determined spectrophotometrically using ϵ (Rhod-DOPE, $\lambda_{\text{max}} = 559 \text{ nm}$, chloroform) = $95 \times 10^3 \text{ M}^{-1} \text{ cm}^{-1}$ (Haugland, 1996). The absorption spectra in vesicle suspensions were corrected for light scattering using the scattering profile obtained in the absence of probe.

2.4. Steady-state fluorescence spectroscopy

Fluorescence steady-state measurements were carried out with an SLM-Aminco 8100 series 2 spectrofluorometer in right angle geometry, the light source being a 450 W Xe arc lamp and the reference a Rhodamine B quantum counter solution. Excitation and emission spectra were corrected using the correction file supplied by the manufacturer. 0.5 cm \times 0.5 cm quartz cuvettes were used. The steady-state anisotropy, $\langle r \rangle$, was calculated from (e.g., (Lakowicz, 2006))

$$\langle r \rangle = \frac{(I_{VV} - GI_{VH})}{(I_{VV} + 2GI_{VH})} \quad (1)$$

where the different intensities I_{ij} are the steady-state vertical and horizontal components of the fluorescence emission with excitation vertical (I_{VV} and I_{VH} , respectively) and horizontal (I_{HV} and I_{HH} , respectively) to the emission axis. The latter pair of components is used to calculate the G factor ($G = I_{HV}/I_{HH}$). Polarization of excitation and emission light was achieved using Glan-Thompson polarizers. Blank subtraction was taken into account for all anisotropy components, as well as for other fluorescence intensity measurements.

2.5. Time-resolved fluorescence spectroscopy

For time-resolved measurements, the instrumentation (single-photon timing technique) consisted of a cavity-dumped dye laser of Rhodamine 6G, synchronously pumped by a mode-locked Ar⁺ laser (514.5 nm, Coherent Innova 200-10). Rhod-DOPE was excited at $\lambda = 575 \text{ nm}$ and its emission at the magic angle was measured at $\lambda = 620 \text{ nm}$ using a Hamamatsu R-2809 MCP photomultiplier. The instrument response functions ($\sim 80 \text{ ps}$ fwhm) for deconvolution were generated from scatter dispersion of colloidal silica in water (Aldrich, Milwaukee, WI). The fluorescence decays were obtained with an accumulation of 20,000 counts in the peak channel, and time-scales ranging from 7.5 ps/channel to 15.3 ps/channel were

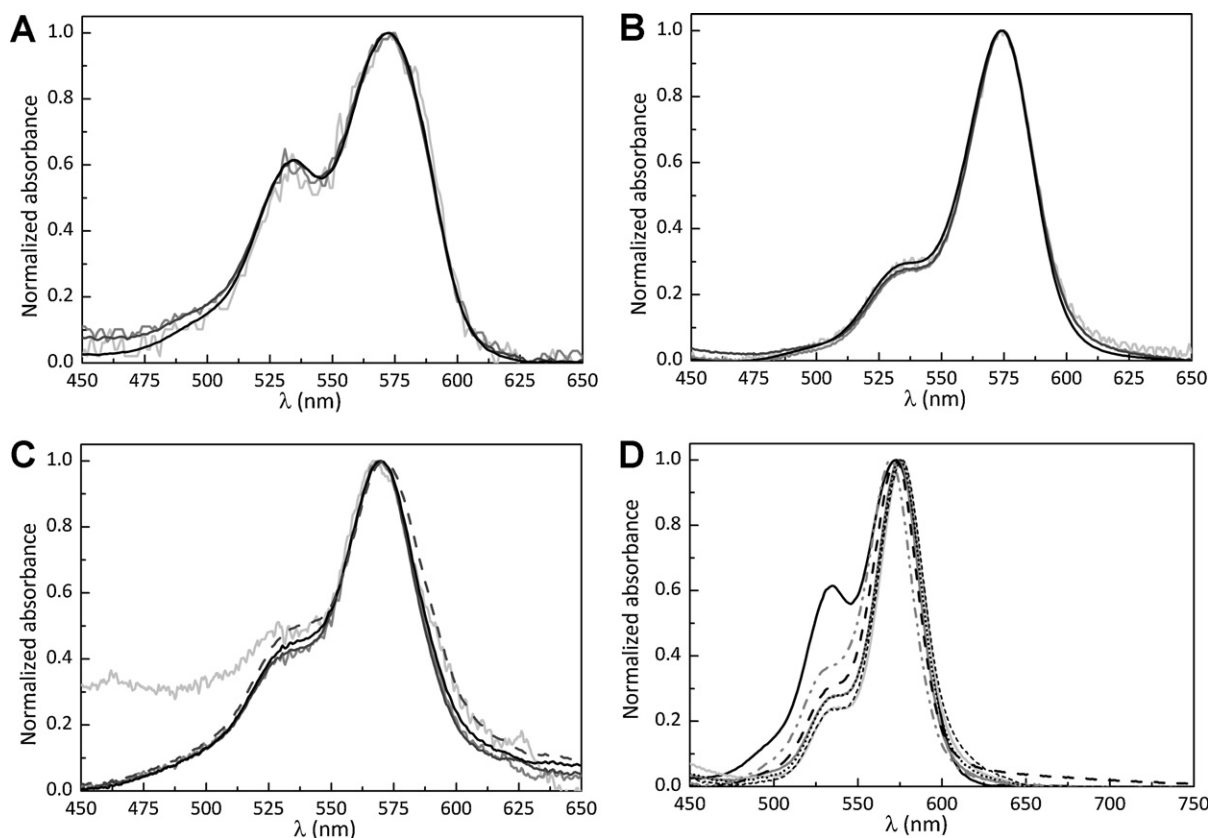


Fig. 1. Normalized Rhod-DOPE absorption spectra at room temperature (24 °C) in (A) buffer (probe concentration of 0.5 μM (light gray), 1.0 μM (gray), 2.5 μM (dark gray), 5.0 μM (black)); (B) DOPC (probe concentration of 0.5 μM (light gray), 2.5 μM (gray), 5.0 μM (dark gray), 20.0 μM (black)) and (C) DPPC/Chol (3:2) (probe concentration of 0.5 μM (light gray), 1.0 μM (gray), 2.5 μM (dark gray), 5.0 μM (black) and 10.0 μM (dashed dark gray) membranes. (D) Normalized absorption spectra of 5.0 μM Rhod-DOPE in buffer (black), DOPC (gray), DOPC/Chol (3:2) (light gray), POPC (dashed black), POPC/Chol (3:2) (dotted black), DPPC/Chol (3:2) (dash dotted gray) and DPPC (small dotted black) membranes.

used. The fluorescence quartz cells had 0.5 cm \times 0.5 cm dimensions. Blank decays were acquired and photon counts were negligible.

The fluorescence intensity decays were described by a sum of exponentials,

$$i(t) = \sum_i \alpha_i \exp(-t/\tau_i) \quad (2)$$

where α_i are the normalized amplitudes, and τ_i , the lifetimes associated to component i of the fluorescence decay. The mean or average lifetime (or intensity averaged lifetime) is given by

$$\langle \tau \rangle = \frac{\sum_i \alpha_i \tau_i^2}{\sum_i \alpha_i \tau_i} \quad (3)$$

and the amplitude-weighted averaged lifetime is defined as

$$\bar{\tau}_i = \sum_i \alpha_i \tau_i \quad (4)$$

(e.g., (Lakowicz, 2006; Sillen and Engelborghs, 1998)). The fluorescence decay analyses (individual and global) were performed using the TRFA software (Scientific Software Technologies Center, Minsk, Belarus) based on the Levenberg–Marquardt algorithm.

3. Results

3.1. Absorption spectroscopy

The absorption spectra of Rhod-DOPE for the systems studied are shown in Fig. 1, normalized to the maximum absorbance. The spectra were acquired at room temperature in: (i) aqueous solution; (ii) l_d membranes composed of DOPC (where phenomena such as probe aggregation are less expected), and (iii) DPPC/Chol

(60:40) membranes in the l_o phase (where stronger alterations in the absorption spectra are reported (MacDonald, 1990)). For each system, two observations are worth mentioning: (i) the vibrational progression of the spectra between 470 and 650 nm did not undergo any significant alteration upon increasing probe concentration; and (ii) the relation between maximum absorbance and probe concentration is linear, in agreement with Beer–Lambert's law (see below). These observations are evidence that in this concentration range there are no changes in the probe aggregation state, since these would likely result in spectral alterations due to excitonic interactions between the Rhod-DOPE molecules (see, e.g. studies by López Arbeloa and coworkers (Bujdák et al., 2006; Chaudhuri et al., 1999; López Arbeloa et al., 2002, 1998)). The shoulder at \sim 525–530 nm presents only minor differences for the DPPC/Chol system at the lower probe concentration. This is due to light scattering artefacts caused by the lipid dispersions, which are more pronounced at shorter wavelengths and in samples with lower absorbance values. However, when comparing Rhod-DOPE spectra in aqueous solution and in lipid membranes (Fig. 1D) there is a striking difference in the shape and amplitude in the shoulder located at shorter wavelengths, which becomes a distinct peak for the probe in water. This difference is consistent with the formation of probe aggregates in aqueous solution (Bujdák et al., 2006; Chaudhuri et al., 1999; López Arbeloa et al., 2002, 1998), possibly due to the micellar arrangement of the probe molecules. Minor differences are observed among the distinct lipid systems, with Rhod-DOPE in DPPC/Chol l_o membranes presenting an intermediate behavior, although no aggregates are formed in this system, as will be shown later on. Those differences are probably due to environmental (polarity) properties specific of each lipid system.

Table 1
Rhod-DOPE molar absorption coefficients (ϵ) and bimolecular rate quenching constants (k_q) determined from the Stern–Volmer relationship (Eq. (5)) and diffusion coefficients (D) calculated from k_q using the Smoluchowski equation with transient effects (Eq. (6)) for the system studied at 24 °C.

| | Lipid phase | $10^3 \epsilon$ ($M^{-1} \text{cm}^{-1}$) | k_q ($\text{mol}^{-1} \text{dm}^3 \text{s}^{-1}$) | D ($\text{cm}^2 \text{s}^{-1}$) |
|-----------------|-------------|---------------------------------------------|-------------------------------------------------------|-------------------------------------|
| DOPC | l_d | 104.8 | 1.82×10^9 | 1.46×10^{-8} |
| POPC | l_d | 99.4 | 1.09×10^{10} | 3.93×10^{-7} |
| DOPC/Chol (3:2) | l_d | 79.5 | 7.32×10^8 | 2.47×10^{-9} |
| POPC/Chol (3:2) | Weak l_o | 89.8 | 8.69×10^9 | 2.66×10^{-7} |
| DPPC/Chol (3:2) | l_o | 46.3 | 1.73×10^{13} | 3.62×10^{-3} |
| DPPC | Gel | 64.8 | 6.66×10^{10} | 6.52×10^{-6} |

In Fig. 2, the maximum absorbance as a function of probe concentration is shown for representative systems. The plots are linear, and from them, the molar absorption coefficients (ϵ) were calculated (Table 1). Between the largest and the smallest value there is only a difference by a factor of ~ 2 , and the highest values are closer to values reported in organic solvent (ϵ (Rhod-DOPE, $\lambda_{\text{max}} = 559 \text{ nm}$, chloroform) = $95 \times 10^3 \text{ M}^{-1} \text{cm}^{-1}$ (Haugland, 1996)). Although the distinct electronic properties displayed by Rhod-DOPE in each lipid system could intuitively result from differences in the hydrophobicity of the environment surrounding the Rhodamine moiety (and in this way polarity and polarizability) from one sample to the other, our results show that there is no obvious relationship between the degree of hydration of the lipid membrane and the molar absorption coefficients of Rhod-DOPE (Table 1). As will be shown later on, the distinctive membrane organization of the probe molecules in each lipid phase is the major factor contributing for Rhod-DOPE photophysics.

3.2. Fluorescence lifetimes and steady-state fluorescence intensity analysis

Previously, it was observed that depending on membrane composition, Rhodamine-based membrane probes can display different trends of fluorescence intensity and lifetime variation upon increments of probe concentration (e.g. (de Almeida et al., 2007; MacDonald, 1990)). Moreover, it was shown that these probes, at a fixed probe:lipid ratio, have different fluorescence lifetimes depending on the lipid phase, and this was used for instance, to calculate their partition coefficient between two lipid phases (e.g. (de Almeida et al., 2005; Loura et al., 2001)). In this work, we performed a systematic study of the variation of the lifetime of the probe Rhod-DOPE for a variety of representative lipid mixtures, as a function of probe:lipid ratio.

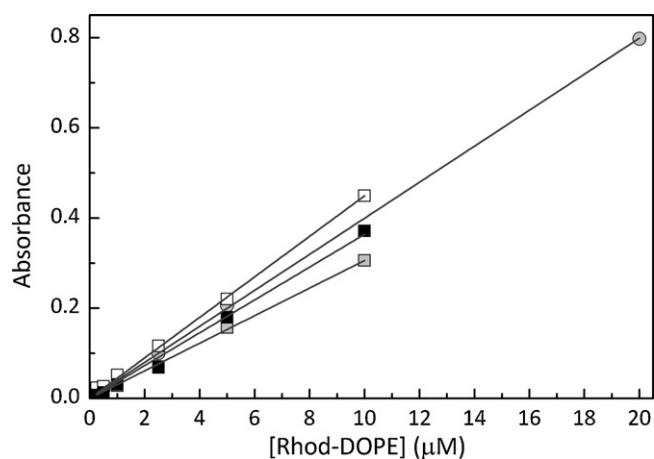


Fig. 2. Maximum absorbance of Rhod-DOPE as a function of probe concentration in DOPC (black symbols), POPC (gray symbols), DPPC/Chol (3:2) (light gray symbols) and DPPC (open symbols) membranes at 24 °C. The solid lines are the linear fit of the Beer–Lambert's law to the experimental data.

In all systems studied, the fluorescence intensity decay of the probe could be described by two or three exponentials (Eq. (2)), though one of the components was dominant for very diluted probe concentrations and its value converged for all samples (not shown). However, in the individual decay analyses it was not feasible to interpret all the components observed, and more attention was paid to the average lifetime ($\langle \tau \rangle$) and amplitude-weighted lifetime ($\bar{\tau}$) (Eqs. (3) and (4), respectively). In Fig. 3, panels A and B, respectively, those parameters are represented for several lipid systems as a function of probe concentration. In general, a decrease of the fluorescence lifetime of the probe with increasing probe:lipid ratio takes place. However, whereas this decrease is very mild for l_d membranes, it is stronger in systems in the gel phase and in the l_o phase. In agreement with previous observations, the decrease of

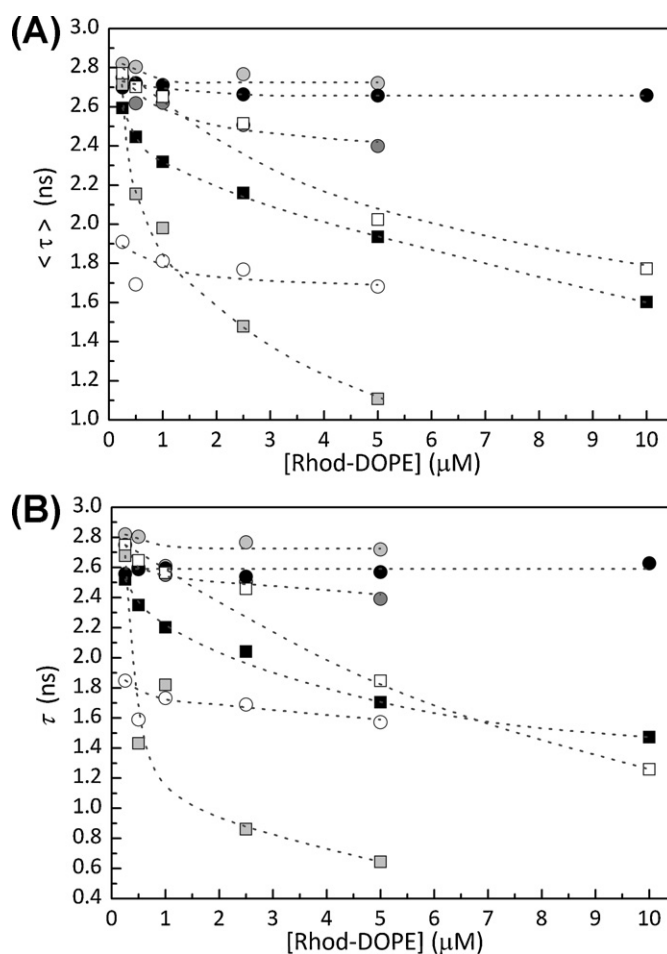


Fig. 3. Rhod-DOPE fluorescence lifetimes as a function of probe concentration at room temperature (24 °C). (A) Mean fluorescence lifetimes ($\langle \tau \rangle$, Eq. (3)) and (B) amplitude-weighted lifetimes ($\bar{\tau}$, Eq. (4)) in buffer (open circles), DOPC (light gray circles), DOPC/Chol (3:2) (gray circles), POPC (solid circles), POPC/Chol (3:2) (open squares), DPPC/Chol (3:2) (gray squares) and DPPC (solid squares) membranes. The dotted lines are merely guides for the eye.

lifetime is accentuated by the presence of cholesterol (de Almeida et al., 2007; MacDonald, 1990). However, for the system DOPC/Chol, where a condensed l_o phase does not form (Davis et al., 2009; de Almeida et al., 2007), there is only a slight decrease in comparison to the DOPC system, and it presents values quite close to the POPC system, a phospholipid in the l_d phase.

Since the absorption data does not support the formation of significant probe aggregates in the lipid membranes, the results obtained in these systems were analyzed in the framework of a self-quenching Stern–Volmer analysis. Hence, the values of $\langle\tau\rangle$ and $\bar{\tau}$ for each system (Fig. 3) were extrapolated to zero concentration of Rhod-DOPE to obtain the average lifetime and amplitude-weighted lifetime of the probe in the absence of self-quenching, $\langle\tau\rangle_0$ and $\bar{\tau}_0$, respectively. A dynamic self-quenching process in a time-resolved fluorescence experiment is described by the Stern–Volmer equation (Sillen and Engelborghs, 1998):

$$\frac{\bar{\tau}_0}{\bar{\tau}} = 1 + k_q \langle\tau\rangle_0 [F] \quad (5)$$

where the subscript 0 indicates infinite dilution, $k_q \langle\tau\rangle_0$ is the Stern–Volmer constant, k_q the bimolecular quenching rate constant and $[F]$ is the fluorophore concentration. In this study, the effective Rhod-DOPE concentration in the membrane was used. This was determined from the molar volumes of DPPC ($V_m = 0.692 \text{ dm}^3/\text{mol}$), POPC ($V_m = 0.761 \text{ dm}^3/\text{mol}$), DOPC ($V_m = 0.780 \text{ dm}^3/\text{mol}$), Chol ($V_m = 0.7 \text{ dm}^3/\text{mol}$), also taking into account Chol condensing effect when appropriate (Cevc and Marsh, 1987; de Almeida et al., 2004). For each system this relationship presented a good linearity (results not shown), even though slight deviations are expected when using the average fluorescence lifetimes (Eq. (3)) to describe multi-exponential decays (Sillen and Engelborghs, 1998). To obtain information about the probe dynamics in each lipid system studied, the bimolecular quenching rate constant was calculated (Table 1). This is related to the diffusion coefficient of the fluorophore (D) via the Smoluchowski equation taking into account transient effects (Umberger and LaMer, 1945):

$$k_q = 4\pi N_A (2R_c)(2D) \left[\frac{1 + 2R_c}{(2\bar{\tau}_0 D)^{1/2}} \right] \quad (6)$$

where N_A is the Avogadro number and R_c the collisional radius. The recovered diffusion coefficients are also listed in Table 1. It can be seen that, whereas for the systems in the l_d phase, the l_d values are those usually found for lipids, probes and proteins in that phase (Chiantia et al., 2006; Dietrich et al., 2001; Vaz et al., 1982), the values obtained in gel and in the typical l_o phase (DPPC/Chol) are higher when in fact they should be lower. In the case of the “weak interaction POPC/Chol l_o phase”, the difference is about one order of magnitude, whereas and for the canonical DPPC/Chol l_o and DPPC gel systems, the D values recovered are several orders of magnitude higher than expected (Chiantia et al., 2006; Dietrich et al., 2001; Vaz et al., 1982). These high values have no physical meaning and are only reporting a strong clustering of the probe in these membranes, as will be discussed further ahead. The Stern–Volmer equation describes fairly well the data for all systems studied, and from its detailed analysis specific information about probe membrane organization in each system is retrieved.

To obtain further information about the molecular events defining Rhod-DOPE photophysics in each lipid phase, the steady-state fluorescence intensity (I_F) was also measured. In Fig. 4, the variation of I_F (corrected for reabsorption and inner filter effects (Lakowicz, 2006)) as a function of Rhod-DOPE concentration is shown for the different lipid systems. In all cases, there is always a negative deviation to linearity, as expected when a dynamic self-quenching

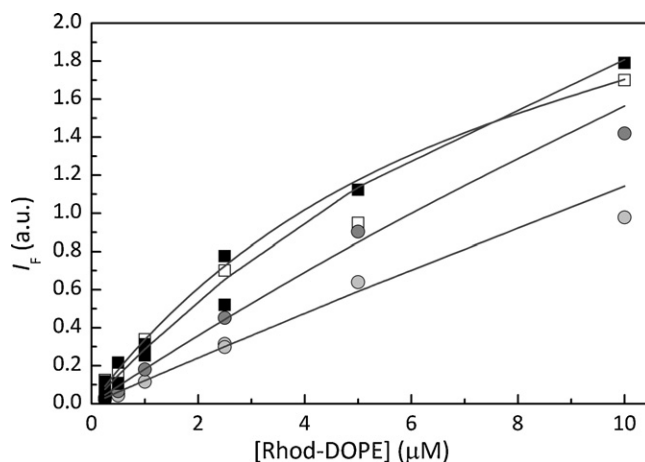


Fig. 4. Rhod-DOPE steady-state fluorescence intensity (I_F) as a function of probe concentration in DOPC (circles), DOPC/Chol (3:2) (triangles), POPC/Chol (3:2) (squares), and DPPC (diamonds) membranes at 24 °C. The lines are the non-linear fit of Eq. (7) to the experimental data, using the parameters presented in Table 1.

process is operative. The following equation was used to describe the I_F data:

$$I_F = \frac{C [F]}{1/\langle\tau\rangle_0 + k_q [F]} \quad (7)$$

where C is a normalization constant. This equation is derived considering only a dynamic self-quenching process, *i.e.* absence of static quenching (Fernandes et al., 2003). In this way, the eventual contribution of a static quenching mechanism for Rhod-DOPE fluorescence decrease could be assessed. As can be verified in Fig. 4, the data is well described by this equation using the parameters retrieved from the time-resolved dynamic self-quenching Stern–Volmer analysis (Table 1). Therefore, any significant contribution of static quenching processes in Rhod-DOPE fluorescence behavior is ruled out.

3.3. Emission depolarization studies

A study of energy homotransfer (energy migration) between Rhod-DOPE molecules was performed to obtain further information about the probe membrane organization in each lipid system. Since energy homotransfer leads to a loss in the polarization of the fluorophore emission without fluorescence quenching (Loura et al., 1996; Prieto et al., 1994), we measured Rhod-DOPE steady-state anisotropy as a function of probe concentration in POPC, POPC/Chol, DPPC/Chol and DPPC membranes (Fig. 5). Also shown, is the theoretical emission depolarization curve expected for a random distribution of fluorophores in 2D in a DPPC gel at 25 °C, according to a Monte-Carlo simulation performed by Snyder and Freire (1982). Such as we observed before (Prieto et al., 1994), the experimental results obtained for this system present a deviation to the theoretical curve. This occurs since the theoretical model assumes a 2D isotropic distribution of the transition moments of the fluorophores, which is not verified in lipid bilayers. In these cases, the fluorophores transition moments are not distributed isotropically, but restricted to a distribution imposed by a “wobbling-in-a-cone” (Prieto et al., 1994).

Between each lipid system studied, Rhod-DOPE does not present significant spectral alterations (so there is similar absorption–emission spectral overlap) (Fig. 1D) nor substantial changes in its fluorescence quantum yield (ϕ) at the lowest probe concentration (Fig. 3B), which could lead to drastic variations in its Förster radius (R_0) for energy homotransfer. Although upon increasing probe concentration, variations in Rhod-DOPE

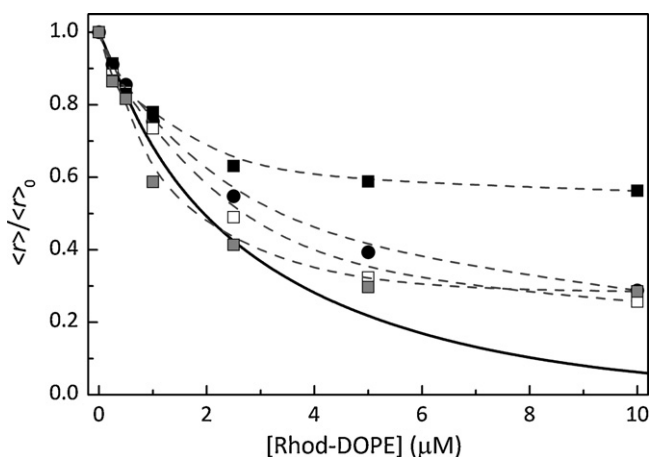


Fig. 5. Ratio of the steady-state fluorescence anisotropy of Rhod-DOPE to its anisotropy at infinite dilution ($\langle r \rangle_0$) as a function of probe concentration in POPC (black circles), POPC/Chol (3:2) (gray circles), DPPC (black squares) and DPPC/Chol (3:2) (gray squares) membranes. Also shown is the theoretical 2D depolarization curve for DPPC at 25 °C (Snyder and Freire, 1982) assuming $R_0 = 64.1 \text{ \AA}$ (Medhage et al., 1992) (solid line). The dotted lines are merely guides for the eye.

fluorescence quantum yield occur, these do not alter significantly the R_0 for energy homotransfer due to its dependence on $\phi^{1/6}$ (e.g. (Loura et al., 1996)). Therefore, R_0 can be considered essentially invariant in each lipid phase and thus, the distinct emission depolarization trends observed for the different lipid membranes can be interpreted in terms of alterations of probe molecules membrane distribution.

In l_d membranes (POPC system), the probe transition moments distribution is quite broad due to the high angle of their rotational cone. Assuming that there is no clustering as the probe concentration is increased (i.e. a random distribution of the probe), it is expected that Rhod-DOPE emission depolarization in this system is the highest. One the other hand, in the DPPC gel phase, where the rotational dynamics of Rhod-DOPE transition moments is more reduced, Rhod-DOPE emission depolarization should be the lowest. However, the trend of Rhod-DOPE emission depolarization will never follow the theoretical curve for this system in the probe concentration range studied due to the reasons discussed above. The expected variation for the l_o systems (DPPC/Chol and POPC/Chol) should be contained within these extremes, l_d and gel phases. Surprisingly, in the l_o systems, the depolarization is still more efficient than the one observed for the l_d system. This can only be explained by probe clustering in the condensed l_o phases. The small distances between the Rhod-DOPE molecules in these clusters promote a more efficient energy homotransfer process that leads to a significant depolarization of the probe emission, overcoming the more restricted dynamics of the probe molecules in l_o phases as compared to the l_d ones. This conclusion about Rhod-DOPE membrane organization is in agreement with those retrieved from the time-resolved Stern–Volmer analysis.

3.4. Rhod-DOPE l_o/l_d partition coefficient in POPC/Chol membranes

Rhod-DOPE phase behavior in membranes displaying different types of phase coexistence, e.g. l_d-l_o , l_d -gel and l_o -gel has already been characterized (de Almeida et al., 2007, 2005; Juhasz et al., 2010, 2011; Silva et al., 2007). However, knowledge about this probe distribution in POPC/Chol membranes displaying fluid–fluid coexistence is still missing. To determine Rhod-DOPE phase partition in POPC/Chol membranes we measured the variation of the probe amplitude-weighted lifetime as a function of membrane

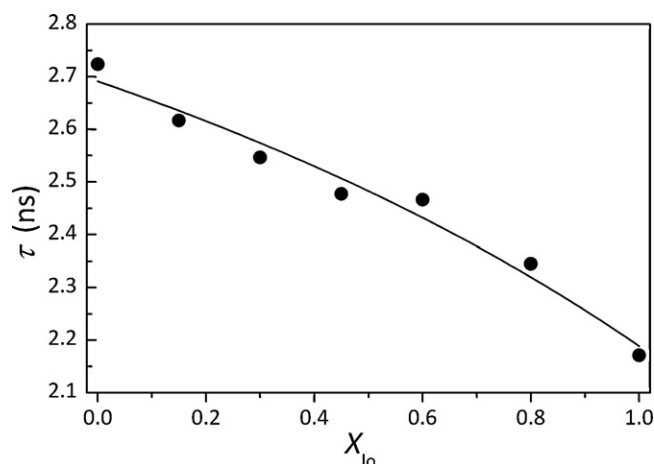


Fig. 6. Amplitude-weighted lifetime of Rhod-DOPE as a function of l_o phase molar fraction in POPC/Chol membranes at 24 °C (de Almeida et al., 2003). The solid line is the non-linear fit of Eq. (8) to the experimental data with $K_p^{l_o/l_d} = 0.7 \pm 0.2$ and $R^2 = 0.974$.

composition (Fig. 6). The mole fraction of each phase was obtained by applying the lever rule to the l_d/l_o phase coexistence tie-line at 24 °C of the POPC/Chol phase diagram (de Almeida et al., 2003). The probe partition coefficient between the “weak interaction l_o ” and l_d phase ($K_p^{l_o/l_d}$), formed in these membranes was determined by fitting the following equation,

$$\bar{\tau} = \frac{\bar{\tau}_{l_o} K_p^{l_o/l_d} X_{l_o} + \bar{\tau}_{l_d} X_{l_d}}{\bar{\tau}_{l_o} X_{l_o} + \bar{\tau}_{l_d} X_{l_d}} \quad (8)$$

to the data. In this expression, $\bar{\tau}_{l_o}$ and X_{l_o} are respectively, the amplitude-weighted lifetime of Rhod-DOPE in the phase i (Eq. (4)) and the mole fraction of that phase. A $K_p^{l_o/l_d} = 0.7 \pm 0.2$ was obtained, showing that the probe has a slight preference for the l_d phase.

4. Discussion

4.1. Rhod-DOPE forms aggregates in water but not in lipid membranes

To fulfill the energetic compliances imposed by the hydrophobic effect, Rhod-DOPE molecules will organize into structures where their hydrophobic aliphatic chains are secluded from water molecules. Due to this process, the solubility of Rhod-DOPE monomers in water will be extremely low, and therefore Rhodamine aggregates will most probably form in a concentration dependent manner. However, in the studied probe concentration range, there are no changes in Rhod-DOPE aggregation state in both aqueous and lipid systems. This is clearly shown by the invariance of the probe absorption spectra upon increasing Rhod-DOPE concentration (Fig. 1). Nonetheless, the absorption spectra of Rhod-DOPE in buffer present evidence for the presence of aggregates, particularly when these are compared to the ones obtained in lipid bilayers (Fig. 1D) or in less polar solvents such as ethanol (data not shown). Rhodamine aggregates are reflected as alterations in the shoulder located at ~ 525 – 530 nm of the probe absorption spectra (Bujdák et al., 2006; Chaudhuri et al., 1999; López Arbeloa et al., 2002, 1998). In buffer this shoulder presents an absorbance that is ~ 0.6 of the maximum absorbance peak (for the $5.0 \mu\text{M}$ concentration), whereas for instance, in POPC membranes this shoulder absorbance is only ~ 0.3 of the maximum. The higher shoulder/peak absorbance ratio observed for buffer is similar to that described for Rhodamine B absorption spectra as the fluorophore molecules progress from a monomeric state in water to an aggregated one in the surface of

smectites clays (Bujdák et al., 2006; Chaudhuri et al., 1999; López Arbeloa et al., 2002, 1998), showing that Rhod-DOPE aggregates are present in buffer. These aggregates are most probably of a micellar nature. In fact, the labeled phospholipid due to the lyssamine Rhodamine B moiety is of an inverted cone shape type. Thus, due to the low critical micellar concentration of long chain phospholipids (in the nanomolar range) (Cevc and Marsh, 1987), Rhod-DOPE micelles can form even for sub-micromolar concentrations of the probe. In a micellar arrangement, the short distances between chromophore groups combines with the hydrophobicity of the Rhodamine B moiety forming sandwich (H-type) aggregates (Cantor and Schimmel, 1980), which results in the observed excitonic alterations of Rhod-DOPE absorption spectra at shorter wavelengths.

Contrary to Rhod-DOPE behavior in buffer, in none of the membrane systems studied there is a compelling evidence for the presence of aggregates. The absorption spectra in membranes are similar to the ones observed in organic solvents (data not shown), presenting a shoulder with an absorbance that is ~ 0.3 of the peak. However, in DPPC/Chol l_0 membranes the shoulder-peak absorbance ratio is raised to ~ 0.4 , indicating that a small fraction of probe aggregates could be forming. Rhodamine aggregates present short fluorescence lifetimes (sub-nanoseconds) or are even non fluorescent (Blackman et al., 2002; Bujdák et al., 2006; López Arbeloa et al., 2002; MacDonald, 1990). Thus, if in DPPC/Chol membranes Rhod-DOPE were extensively aggregating, this should be reflected in the probe fluorescence lifetimes even at the lower concentration, which according to the reasons mentioned previously, should present shorter lifetimes than Rhod-DOPE lifetimes in the remaining lipid systems. However, the probe fluorescence lifetime and amplitude-weighted lifetime for the diluted samples only present slight variations between each of the lipid systems studied, being significantly longer than the one in buffer, where aggregation does occur (Fig. 3). Moreover, Rhod-DOPE steady-state fluorescence intensity data as a function of probe concentration in all systems is well described by a Stern–Volmer analysis, *i.e.* taking into account only a dynamic self-quenching process (Fig. 4). This rules out the formation of probe aggregates in DPPC/Chol l_0 membranes. As will be discussed below, the distinct electronic properties displayed by Rhod-DOPE in this system is a result of the specific probe membrane organization in l_0 phases.

4.2. Rhod-DOPE presents unique photophysical properties in l_0 membranes

At variance with electronic absorption spectra, Rhod-DOPE time-resolved fluorescence data presents noteworthy differences between each of the systems studied (Fig. 3). In general, the probe fluorescence lifetime decreases upon increasing its concentration. However, whereas in buffer and l_d membranes the extent of fluorescence lifetime decrease is low, in l_0 and gel membranes it is more pronounced. These results are not in agreement with the previously description that attributed Rhodamine-lipid enhanced fluorescence self-quenching in lipid membranes to the presence of Chol (MacDonald, 1990).

To understand the underlying mechanism(s) beneath Rhod-DOPE enhanced fluorescence self-quenching in lipid bilayers, the lateral diffusion coefficient of the probe (Table 1) was calculated with the parameters retrieved from the Stern–Volmer analysis of fluorescence lifetimes (Eq. (6)). For membranes in the l_d phase, including one that contains Chol (DOPC/Chol system), the values are similar to those typical for membrane lipid and protein diffusion in the l_d phase ($D = 10\text{--}70 \times 10^{-9} \text{ cm}^2 \text{ s}^{-1}$ (Chiantia et al., 2006; Dietrich et al., 2001; Vaz et al., 1982)). Moreover, there is a good agreement between the time-resolved and steady-state data (Fig. 4), *i.e.* it is possible to describe the variation of the fluorescence intensity without invoking fluorescence static quenching

contributions, *e.g.*, sphere of action or ground-state complex formation (de Almeida et al., 2004). Thus, Rhod-DOPE fluorescence self-quenching in l_d membranes results solely from an increase in the probe membrane concentration, which increases the probability of collision between two probe molecules during their excited state. These results, together with the absorption data unequivocally show that in l_d systems, Rhod-DOPE is mainly monomeric and presents a random membrane distribution. This is in agreement with the analysis of the steady-state anisotropy data performed for the same probe in l_d membranes composed of POPC/palmitoyl-sphingomyelin/Chol, for probe:lipid ratios of 1:200 and 1:500 (de Almeida et al., 2005).

Rhod-DOPE photophysical behavior in l_d membranes contrasts with that obtained in gel and l_0 phases. The time-resolved fluorescence Stern–Volmer analysis clearly show that the probe lifetime decrease in these systems cannot be explained exclusively by a dynamic self-quenching mechanism considering random probe distribution, since the diffusion coefficients calculated within this framework for DPPC and DPPC/Chol membranes are higher than expected (Table 1). Thus, other processes must be invoked to explain the decrease of the probe fluorescence lifetime with the increase in the probe:lipid ratio. Previous studies have shown that Rhodamine monomer–dimer hetero-FRET can lead to a decrease in the probe fluorescence lifetime (Blackman et al., 2002; MacDonald, 1990). However, neither the absorption data nor the steady-state Stern–Volmer analysis support the formation of probe aggregates, even at the highest probe concentration, therefore invalidating this hypothesis. In this way, the formation of probe-rich membrane regions, *i.e.* Rhod-DOPE clusters (although not leading to probe aggregation), in gel and l_0 membranes explains the results. The surface of gel membranes generally presents nanometer sized defect lines, where the molecular architecture is strongly less ordered as the bulk membrane (though not as disordered as the fluid) (*e.g.*, (Loura et al., 1996)). Rhod-DOPE insertion in the compact gel phase formed by DPPC molecules is surely hindered by its bulky Rhodamine moiety. Therefore, probe partitioning to less ordered regions such as defect lines will be favored. Due to the small area of the defects, high local Rhod-DOPE concentrations are expected. This feature combined with the less ordered environment of those regions, increases the interaction probability between probe molecules during their excited state, leading to an enhanced fluorescence self-quenching.

In l_0 membranes, a similar process as the one described above also occurs. Although, in this case, owing to the unique biophysical properties of these membranes, Rhod-DOPE molecules concentrate into membrane nanodomains. The fluid nature of the membrane renders probe molecules a high lateral diffusion coefficient, several magnitudes higher than in gel defects, resulting in a self-quenching mechanism even more efficient than in those defect lines. This is clearly demonstrated by the stronger shortening of Rhod-DOPE fluorescence lifetime in DPPC/Chol membranes as compared to pure DPPC gel ones, which allows the recovering of unrealistic diffusion coefficients differing in several orders of magnitude (Table 1). However, both the fluorescence lifetime and steady-state intensity were described by the Stern–Volmer equation. This is because the relationship is still valid but the fluorophore concentration, $[F]$ in Eq. (7), should be replaced by its effective concentration which is higher.

Further evidence for the organization of Rhod-DOPE molecules into probe-rich membrane nanodomains in l_0 membranes, is obtained from energy homotransfer studies (Fig. 5). As expected, in none of the lipid phase systems studied (l_d , l_0 and gel), the experimental results follow the theoretical depolarization curve for a 2D isotropic distribution of fluorophores (Snyder and Freire, 1982), due to the anisotropic distribution of the probe transition moments when in lipid membranes, as already discussed.

Nevertheless, and contrary to what it would be expected, Rhod-DOPE depolarization emission data in l_o membranes does not lay within the probe depolarization values for gel and l_d membranes. In fact, in this system, the probe presents the highest extent of emission depolarization, which can only be explained by the existence of very efficient energy migration between Rhod-DOPE molecules. This implies the formation of probe clusters, which correspond to the probe-rich membrane regions mentioned above. In these nanodomains, the small distances between Rhod-DOPE molecules, in addition to their small Stokes shift, high quantum yield and high molar absorption coefficient promote an efficient energy migration process. Therefore, it seems that cluster formation is underneath Rhod-DOPE enhanced self-quenching in l_o membranes, being an exclusive feature of this type of lipid phases.

Being a 1,2-unsaturated acyl chain and bulky headgroup lipid, the energy cost of inserting Rhod-DOPE molecules into ordered membrane regions is high. For this reason, Rhod-DOPE presents a preferential localization into less ordered membrane domains (see above and e.g. (de Almeida et al., 2007; Juhasz et al., 2010, 2011; Silva et al., 2007)). In gel membranes, Rhod-DOPE molecules preferentially localize into the less ordered defect lines that corrugate the membrane surface. Since these disordered membrane regions are not present in l_o membranes, Rhod-DOPE molecules cluster into probe-rich domains, where the local order is lower than the bulk membrane. Cluster formation is preceded by the insertion of Rhod-DOPE molecules into a membrane region, where it locally decreases the order of lipid acyl chains, in this way creating a more suitable environment for other Rhod-DOPE molecules, leading to probe clustering, in a similar way as described for γ M4 transmembrane domain-rich patch formation in l_o membranes (de Almeida et al., 2004). This environment may also be related to the membrane dipole potential, as this has also been described as a biophysical property of Chol-enriched membranes that prevent Rhodamine-based probe efficient incorporation into l_o phases, even in cases where the acyl chains of the probe are saturated (Estronca et al., 2002). For these reasons and the additional arguments already described, Rhod-DOPE fluorescence lifetimes present a marked decrease with increasing probe concentration in condensed l_o phases. Not surprisingly, the magnitude of these processes is highly dependent on the lipids that compose the l_o phase, being higher for lipids that promote more compact phases. This is clearly seen by the stronger Rhod-DOPE fluorescence lifetime decrease in canonical l_o DPPC/Chol as compared to the “weak interaction l_o ” POPC/Chol.

4.3. Rhod-DOPE membrane lateral distribution in POPC/Chol membranes

As already mentioned, an accurate interpretation of the data of fluorescent probes in complex membrane systems can only be achieved if their photophysical properties and membrane lateral organization are known. To complement the knowledge of Rhod-DOPE behavior in membranes presenting phase coexistence (e.g. (de Almeida et al., 2007; Juhasz et al., 2010, 2011; Silva et al., 2007)), we measured the probe partition coefficient between the “weak interaction l_o ” and l_d phases formed in POPC/Chol membranes (Fig. 6). The value obtained ($K_p^{l_o/l_d} = 0.7 \pm 0.2$) is in accordance with the higher preference for fluid-disordered phases reported for this probe in DOPC/DPPC mixtures ($K_p^{gel/l_d} = 0.2 \pm 0.5$) (de Almeida et al., 2007) and also in POPC/sphingomyelin/Chol model raft membranes ($K_p^{l_o/l_d} = 0.3 \pm 0.1$) (de Almeida et al., 2005; Silva et al., 2007). Interestingly, it also shows that the molecular condensation of the “weak interaction l_o ” phase formed in POPC/Chol mixtures is high enough to hamper the insertion of the double acyl unsaturated

chains and bulky headgroup fluorescent lipid in this condensed phase.

5. Conclusions

The thorough characterization of Rhod-DOPE absorption and fluorescence behavior in aqueous and in different lipid environments allowed us to establish a relation between the probe photophysical properties and membrane state. This information was supplemented with information from probe lateral distribution in POPC/Chol membranes, contributing for the completion of Rhod-DOPE phase behavior and phase-related fluorescence properties in different lipid systems (e.g. (de Almeida et al., 2007; Juhasz et al., 2010, 2011; Silva et al., 2007)). Moreover, the underlying mechanism of Rhod-lipids enhanced self-quenching in membranes could be unraveled using the method employed. Our results clearly show that this specific behavior of Rhodamine probes is a result of the exceptional environment of the condensed l_o phases, and not merely due to Chol presence in the lipid membranes, as previously described (MacDonald, 1990). Owing to the unique photophysical properties of this probe in l_o phases, which is intimately related with lipid rafts cell membranes state (Stockl et al., 2008), this probe presents a high potential in the study of the structural and functional significances of these special domains not only in membrane model systems, but also in cells.

Acknowledgments

This work was supported by Fundação para a Ciência e Tecnologia grants PTDC/QUI-BIQ/099947/2008 and PTDC/QUI-BIQ/112067/2009 and fellowship BD/36635/2007 (B.M.C.).

References

- Aroeti, B., Henis, Y.L., 1987. Fusion of native Sendai virions with human erythrocytes. Quantitation by fluorescence photobleaching recovery. *Exp. Cell Res.* 170, 322–337.
- Bagatolli, L.A., Gratton, E., 2000. Two photon fluorescence microscopy of coexisting lipid domains in giant unilamellar vesicles of binary phospholipid mixtures. *Biophys. J.* 78, 290–305.
- Bagatolli, L.A., Ipsen, J.H., Simonsen, A.C., Mouritsen, O.G., 2010. An outlook on organization of lipids in membranes: searching for a realistic connection with the organization of biological membranes. *Prog. Lipid Res.* 49, 378–389.
- Bastos, A.E.P., Scolari, S., Stöckl, M., de Almeida, R.F.M., 2012. Applications of fluorescence lifetime spectroscopy and imaging to lipid domains in vivo. *Methods Enzymol.* 504, 57–81.
- Blackman, M.J., Corrie, J.E., Croney, J.C., Kelly, G., Eccleston, J.F., Jameson, D.M., 2002. Structural and biochemical characterization of a fluorogenic rhodamine-labeled malarial protease substrate. *Biochemistry* 41, 12244–12252.
- Bujdák, J., Martínez Martínez, V., López Arbeloa, F., Iyi, N., 2006. Spectral properties of rhodamine 3B adsorbed on the surface of montmorillonites with variable layer charge. *Langmuir* 23, 1851–1859.
- Cantor, R.C., Schimmel, P.R., 1980. Part II: Techniques for the Study of Biological Structure and Function, 1st ed. W.H. Freeman and Company, New York.
- Castro, B.M., de Almeida, R.F., Goormaghtigh, E., Fedorov, A., Prieto, M., 2011. Organization and dynamics of Fas transmembrane domain in raft membranes and modulation by ceramide. *Biophys. J.* 101, 1632–1641.
- Cevc, G., Marsh, D., 1987. Phospholipids Bilayers: Physical Principles and Models. John Wiley and Sons, New York.
- Chaudhuri, R., López Arbeloa, F., López Arbeloa, I., 1999. Spectroscopic characterization of the adsorption of rhodamine 3B in hectorite. *Langmuir* 16, 1285–1291.
- Chiantia, S., Kahya, N., Ries, J., Schwille, P., 2006. Effects of ceramide on liquid-ordered domains investigated by simultaneous AFM and FCS. *Biophys. J.* 90, 4500–4508.
- Davis, J.H., Clair, J.J., Juhasz, J., 2009. Phase equilibria in DOPC/DPPC-d62/cholesterol mixtures. *Biophys. J.* 96, 521–539.
- de Almeida, R.F., Borst, J., Fedorov, A., Prieto, M., Visser, A.J., 2007. Complexity of lipid domains and rafts in giant unilamellar vesicles revealed by combining imaging and microscopic and macroscopic time-resolved fluorescence. *Biophys. J.* 93, 539–553.
- de Almeida, R.F., Fedorov, A., Prieto, M., 2003. Sphingomyelin/phosphatidylcholine/cholesterol phase diagram: boundaries and composition of lipid rafts. *Biophys. J.* 85, 2406–2416.

- de Almeida, R.F., Loura, L.M., Fedorov, A., Prieto, M., 2005. Lipid rafts have different sizes depending on membrane composition: a time-resolved fluorescence resonance energy transfer study. *J. Mol. Biol.* 346, 1109–1120.
- de Almeida, R.F., Loura, L.M., Prieto, M., Watts, A., Fedorov, A., Barrantes, F.J., 2004. Cholesterol modulates the organization of the gammaM4 transmembrane domain of the muscle nicotinic acetylcholine receptor. *Biophys. J.* 86, 2261–2272.
- Dietrich, C., Bagatolli, L.A., Volovyk, Z.N., Thompson, N.L., Levi, M., Jacobson, K., Gratton, E., 2001. Lipid rafts reconstituted in model membranes. *Biophys. J.* 80, 1417–1428.
- Estronca, L.S.M.B.B., João Moreno, M., Abreu, M.S.C., Melo, E., Vaz, W.L.C., 2002. Solubility of amphiphiles in membranes: influence of phase properties and amphiphile head group. *Biochem. Biophys. Res. Commun.* 296, 596–603.
- Fernandes, F., Loura, L.M., Prieto, M., Koehorst, R., Spruijt, R.B., Hemminga, M.A., 2003. Dependence of M13 major coat protein oligomerization and lateral segregation on bilayer composition. *Biophys. J.* 85, 2430–2441.
- Haugland R., 1996. *Handbook of Fluorescent Probes and Research Chemicals*. Molecular Probes, Eugene, OR.
- Hoekstra, D., Klappe, K., 1986. Use of a fluorescence assay to monitor the kinetics of fusion between erythrocyte ghosts, as induced by Sendai virus. *Biosci. Rep.* 6, 953–960.
- Juhasz, J., Davis, J.H., Sharom, F.J., 2010. Fluorescent probe partitioning in giant unilamellar vesicles of 'lipid raft' mixtures. *Biochem. J.* 430, 415–423.
- Juhasz, J., Davis, J.H., Sharom, F.J., 2011. Fluorescent probe partitioning in GUVs of binary phospholipid mixtures: implications for interpreting phase behavior. *Biochim. Biophys. Acta* 1818, 19–26.
- Lakowicz, J.R., 2006. *Principles of Fluorescence Spectroscopy*. Springer, New York.
- López Arbeloa, F., Chaudhuri, R., Arbeloa López, T., López Arbeloa, I., 2002. Aggregation of rhodamine 3B adsorbed in Wyoming montmorillonite aqueous suspensions. *J. Colloid Interface Sci.* 246, 281–287.
- López Arbeloa, F., Herrán Martínez, J.M., López Arbeloa, T., López Arbeloa, I., 1998. The hydrophobic effect on the adsorption of rhodamines in aqueous suspensions of smectites. The rhodamine 3B/laponite B system. *Langmuir* 14, 4566–4573.
- Loura, L.M., Fedorov, A., Prieto, M., 1996. Resonance energy transfer in a model system of membranes: application to gel and liquid crystalline phases. *Biophys. J.* 71, 1823–1836.
- Loura, L.M., Fedorov, A., Prieto, M., 2001. Fluid–fluid membrane microheterogeneity: a fluorescence resonance energy transfer study. *Biophys. J.* 80, 776–788.
- MacDonald, R.I., 1990. Characteristics of self-quenching of the fluorescence of lipid-conjugated rhodamine in membranes. *J. Biol. Chem.* 265, 13533–13539.
- McClare, C.W., 1971. An accurate and convenient organic phosphorus assay. *Anal. Biochem.* 39, 527–530.
- Medhage, B., Mukhtar, E., Kalman, B., Johansson, L.B.A., Molotkovsky, J.G., 1992. Electronic energy transfer in anisotropic systems. Part 5. Rhodamine-lipid derivatives in model membranes. *J. Chem. Soc., Faraday Trans.* 88, 2845–2851.
- Prieto, M.J., Castanho, M., Coutinho, A., Ortiz, A., Aranda, F.J., Gomez-Fernandez, J.C., 1994. Fluorescence study of a derivatized diacylglycerol incorporated in model membranes. *Chem. Phys. Lipids* 69, 75–85.
- Reyes Mateo, C., Brochon, J.C., Pilar Lillo, M., Ulises Acuña, A., 1993. Lipid clustering in bilayers detected by the fluorescence kinetics and anisotropy of trans-parinaric acid. *Biophys. J.* 65, 2237–2247.
- Sillen, A., Engelborghs, Y., 1998. The correct use of average fluorescence parameters. *Photochem. Photobiol.* 67, 475–486.
- Silva, L.C., de Almeida, R.F., Castro, B.M., Fedorov, A., Prieto, M., 2007. Ceramide-domain formation and collapse in lipid rafts: membrane reorganization by an apoptotic lipid. *Biophys. J.* 92, 502–516.
- Simons, K., Gerl, M.J., 2010. Revitalizing membrane rafts: new tools and insights. *Nat. Rev. Mol. Cell Biol.* 11, 688–699.
- Snyder, B., Freire, E., 1982. Fluorescence energy transfer in two dimensions. A numeric solution for random and nonrandom distributions. *Biophys. J.* 40, 137–148.
- Stegmann, T., Hoekstra, D., Scherphof, G., Wilschut, J., 1986. Fusion activity of influenza virus. A comparison between biological and artificial target membrane vesicles. *J. Biol. Chem.* 261, 10966–10969.
- Stockl, M., Plazzo, A.P., Korte, T., Herrmann, A., 2008. Detection of lipid domains in model and cell membranes by fluorescence lifetime imaging microscopy of fluorescent lipid analogues. *J. Biol. Chem.* 283, 30828–30837.
- Umberger, J.Q., LaMer, V.K., 1945. The kinetics of diffusion controlled molecular and ionic reactions in solution as determined by measurements of the quenching of fluorescence. *J. Am. Chem. Soc.* 67, 1099–1109.
- van Meer, G., 2005. Cellular lipidomics. *EMBO J.* 24, 3159–3165.
- Vaz, W.L., Criado, M., Madeira, V.M., Schoellmann, G., Jovin, T.M., 1982. Size dependence of the translational diffusion of large integral membrane proteins in liquid-crystalline phase lipid bilayers. A study using fluorescence recovery after photobleaching. *Biochemistry* 21, 5608–5612.
- Vist, M.R., Davis, J.H., 1990. Phase equilibria of cholesterol/dipalmitoylphosphatidylcholine mixtures: 2H nuclear magnetic resonance and differential scanning calorimetry. *Biochemistry* 29, 451–464.